

## X-ray absorption branching ratio in actinides: LDA+DMFT approach

This article has been downloaded from IOPscience. Please scroll down to see the full text article.

2009 EPL 85 17007

(<http://iopscience.iop.org/0295-5075/85/1/17007>)

View [the table of contents for this issue](#), or go to the [journal homepage](#) for more

Download details:

IP Address: 128.6.224.225

The article was downloaded on 24/06/2010 at 05:59

Please note that [terms and conditions apply](#).

# X-ray absorption branching ratio in actinides: LDA + DMFT approach

J. H. SHIM<sup>(a)</sup>, K. HAULE and G. KOTLIAR

*Department of Physics, Rutgers University - Piscataway, NJ 08854, USA*

received 23 September 2008; accepted in final form 3 December 2008  
published online 16 January 2009

PACS 78.70.Dm – X-ray absorption spectra

PACS 71.10.-w – Theories and models of many-electron systems

PACS 71.27.+a – Strongly correlated electron systems; heavy fermions

**Abstract** – To investigate the X-ray absorption (XAS) branching ratio from the core  $4d$  to valence  $5f$  states, we set up a theoretical framework by using a combination of density functional theory in the Local Density Approximation and Dynamical Mean-Field Theory (LDA + DMFT), and apply it to several actinides. The results of the LDA + DMFT reduces to the band limit for itinerant systems and to the atomic limit for localized  $f$  electrons, meaning a spectrum of  $5f$  itinerancy can be investigated. Our results provides a consistent and unified view of the XAS branching ratio for all elemental actinides, and is in good overall agreement with experiments.

Copyright © EPLA, 2009

Understanding the physics of elemental actinide solids is an important issue for many-body physics as well as for applications in nuclear power generation. In the early actinides, the  $f$  electrons behave as waves delocalized through the crystal, while in the late actinides, the  $f$  electrons behave as particles localized around each atom. Plutonium is near the localization-delocalization edge separating these two regimes. X-ray absorption (XAS) from the core  $4d$  to the valence  $5f$  in conjunction with atomic physics calculations has been a powerful probe of the evolution of the valence and the strength of the spin-orbit coupling across the actinide series.

A large number of spectroscopies have been applied to this problem. For example, photoemission spectroscopy of Pu, has revealed a multiple-peak structure in the occupied part of the density of states [1–3]. A combination approach of Local Density Approximation (LDA) and Dynamical Mean-Field Theory (LDA + DMFT) has allowed the interpretation of these features in terms of  $f$  electrons which are delocalized at low frequencies with a mixed valence electron count [4]. Other interpretations of Pu spectroscopies using LDA + DMFT with other impurity solvers have been presented recently [5–7].

High-energy probes such as electron energy-loss spectroscopy (EELS) or X-ray absorption spectroscopy (XAS) constitute a different set of spectroscopies which have been intensively used to study the electronic structure

of the actinide series [8–14]. These experimental works, combined with theoretical calculations exploiting a powerful sum rule, and the electronic structure of the atom has yielded valuable insights on the degree of localization of valence  $5f$  electrons in actinides [8–10] as well as the spin-orbit strength [8,10,11].

Here we address the computation of the branching ratio within DMFT. There are several motivations for this study. 1) While the atomic multiplet approach of ref. [12] describes very successfully the majority of the data in the late actinides, it is restricted to the case that the  $f$  electrons are strictly localized. It is therefore useful to extend this approach by embedding it in a more general method that captures the itinerant limit as well. 2) Many other spectroscopies of the actinides such as photoemission spectroscopies are not well described by a localized model. LDA + DMFT provides a unified picture which reconciles the results of high-energy and low-energy spectroscopies. In physical terms, DMFT can describe the low-energy part of the excitations as itinerant, and the high-energy excitations as localized. Different spectroscopies weight different parts of the spectra. It is useful to incorporate the XAS branching ratio in the general LDA + DMFT formalism to achieve a unified interpretation of high-energy and low-energy spectroscopies. 3) The branching ratio can be expressed as a ratio of two quantities, one involving the spin-orbit coupling and the other involving the  $f$  occupation. Therefore a proper theoretical interpretation of the experiments requires the evaluation of these two

<sup>(a)</sup>E-mail: jishim@physics.rutgers.edu

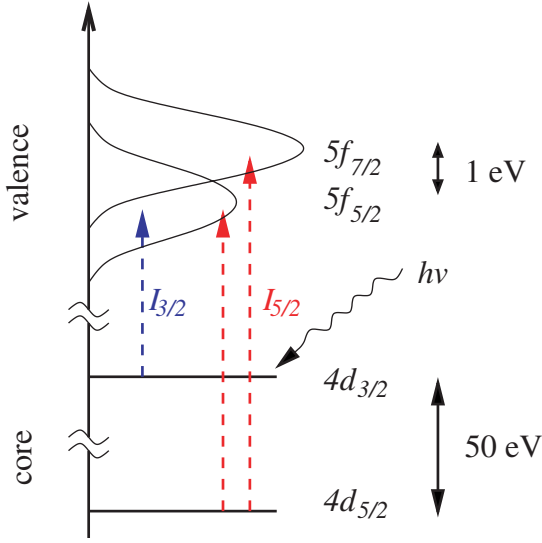


Fig. 1: Schematic diagram of the XAS from core  $4d$  to valence  $5f$  transition. The absorption intensities  $I_{5/2}$  and  $I_{3/2}$  correspond to the  $4d_{5/2} \rightarrow 5f_{5/2,7/2}$  and  $4d_{3/2} \rightarrow 5f_{5/2}$  transitions, respectively. The core levels are clearly discretized by the  $4d_{3/2}$  and  $4d_{5/2}$  levels, but the valence levels are overlapped between the  $5f_{5/2}$  and  $5f_{7/2}$  level due to multiplet splittings and electron itinerancy.

quantities. Until now, experimentally the occupancies were determined to be in an interval of allowed values. XAS and EELS experiments were used to constrain the variations of the spin-orbit coupling for that range of occupancies.

Figure 1 shows a schematic diagram of the  $4d \rightarrow 5f$  transition in XAS. K. Moore and collaborators have shown that EELS experiments give equivalent information [15,16]. One envisions a large splitting due to spin-orbit coupling of the core levels. The electric-dipole selection rule ( $\Delta j = 0, \pm 1$ ), gives rise to two absorption lines:  $I_{5/2}$  ( $4d_{5/2} \rightarrow 5f_{5/2,7/2}$ ) and  $I_{3/2}$  ( $4d_{3/2} \rightarrow 5f_{5/2}$ ). The branching ratio  $B$  is defined by  $B = I_{5/2}/(I_{5/2} + I_{3/2})$ .

When the spin-orbit splitting in the valence band is negligible in comparison with the different sources of broadening (due to multiplet splittings or electron itinerancy) shown schematically in fig. 1, we can neglect the spin-orbit splitting in the final states and the branching ratio  $B$  is given by a statistical value of  $3/5$ , which reflects the relative degeneracies of the initial states. Hence the branching ratio is a probe of the strength of the spin-orbit coupling [8,10,11].

Detail calculations based on the isolated atomic model were shown to be consistent with the experimental result of the late actinides. However, deviations get larger when the system becomes delocalized as in U and Np. Due to the delocalization, the spin-orbit strength is apparently suppressed. We will show that although LDA is a proper approximation for describing many properties of itinerant system, it underestimates the experimental results of early

actinides. So more realistic theoretical model, which can treat both the atomic and itinerant physics, is needed. The LDA + DMFT method is the most promising method for this purpose.

The spin-orbit sum-rule has been fully derived in the pioneering work of van der Laan, Thole and collaborators [12,17–19], and applied to numerous systems. (For recent review, see ref. [15].) Here we summarize the main steps of their derivation, indicating the places where the atoms are considered in a solid-state environment, and where a treatment going beyond band theory and atomic multiplet physics, such as the DMFT method is required.

The X-ray absorption resulting from a core-valence transition, is described by a term in the Hamiltonian that couples the electromagnetic field to a transition operator  $T_q$ , which in the electric dipole approximation is given by

$$T_q = \sum_i T_q(i), \quad (1)$$

$T_q(i)$  is the atomic operator at site  $i$ . We consider transition from a core level denoted by  $j_c (= l_c \pm s)$  to the partially occupied valence levels denoted by  $j_v (= l_v \pm s)$  with absorption of  $q$  polarized light.

$$T_q(i) = \sum_{m_v m_c} \langle l_v s; j_v m_v | \mathbf{r}_q | l_c s; j_c m_c \rangle f_{j_v m_v}^\dagger d_{j_c m_c}, \quad (2)$$

where  $d_{j_c m_c}$  is the annihilation operator of a core electron and  $f_{j_v m_v}^\dagger$  is the creation operator of a valence electron.

The matrix element can be given as a product of a reduced matrix element containing a radial integral and an angular dependent part [20].

$$\begin{aligned} \langle l_v s; j_v m_v | \mathbf{r}_q | l_c s; j_c m_c \rangle &= (-1)^{j_v - j_c} [l_v l_c j_c]^{1/2} \\ &\times \begin{Bmatrix} j_c & 1 & j_v \\ l_v & s & l_c \end{Bmatrix} \begin{pmatrix} j_c & 1 & j_v \\ m_c & q & -m_v \end{pmatrix} \langle l_v s \| \mathbf{r} \| l_c s \rangle, \end{aligned} \quad (3)$$

where  $[a, b, \dots]$  is shorthand for  $(2a+1)(2b+1)\dots$ . Here, we used the Wigner-Eckart theorem. Because we are interested in the transition of given core ( $l_c$ ) and valence ( $l_v$ ) states, we will omit the reduced matrix element below.

When we consider the isotropic spectrum, where the light polarizations are averaged, the absorption intensity summed over the final states  $|f\rangle$  from a many-electron ground state  $|g\rangle$  is

$$\begin{aligned} I &= \sum_q \sum_f \langle g | T_q^\dagger | f \rangle \langle f | T_q | g \rangle \\ &= \sum_q \sum_{m_v m'_v} \sum_{m_c m'_c} \langle d_{j_c m'_c}^\dagger f_{j_v m'_v} f_{j_v m_v}^\dagger d_{j_c m_c} \rangle \\ &\quad \times \langle l_c s; j_c m'_c | \mathbf{r}_q | l_v s; j_v m'_v \rangle \langle l_v s; j_v m_v | \mathbf{r}_q | l_c s; j_c m_c \rangle. \end{aligned} \quad (4)$$

Here we assume that the interference terms ( $\langle T_q(i) T_q(j) \rangle$ ,  $i \neq j$ ) are negligible which is a valid assumption when the core electron states are effectively localized. Since  $|g\rangle$  does not contain holes in the core level, the core shell operators

are removed by  $d_{j_c m'_c}^\dagger |g\rangle = 0$ , and the creation-annihilation term in the intensity can be obtained as

$$\langle d_{j_c m'_c}^\dagger f_{j_v m'_v} f_{j_v m_v}^\dagger d_{j_c m_c} \rangle = \langle f_{j_v m'_v} f_{j_v m_v}^\dagger \rangle \delta_{m_c m'_c}, \quad (5)$$

where we neglected the core-valence interaction, which is a reasonable approximation in  $4d \rightarrow 5f$  transition [8].

Combining eqs. (3)–(5), the the dipole transition probability is

$$\begin{aligned} I &= [l_v l_c j_c] \left\{ \begin{matrix} j_c & 1 & j_v \\ l_v & s & l_c \end{matrix} \right\}^2 \sum_{m_v m'_v} \langle f_{j_v m'_v} f_{j_v m_v}^\dagger \rangle \\ &\times \sum_{m_c q} \begin{pmatrix} j_c & 1 & j_v \\ m_c & q & -m_v \end{pmatrix} \begin{pmatrix} j_c & 1 & j'_v \\ m_c & q & -m'_v \end{pmatrix} \\ &= [l_v l_c j_c] \left\{ \begin{matrix} j_c & 1 & j_v \\ l_v & s & l_c \end{matrix} \right\}^2 \langle n_{j_i}^h \rangle. \end{aligned} \quad (6)$$

We have used the normalization condition.

$$\sum_{m_c q} \begin{pmatrix} j_c & 1 & j_v \\ m_c & q & -m_v \end{pmatrix} \begin{pmatrix} j_c & 1 & j'_v \\ m_c & q & -m'_v \end{pmatrix} = [j_v]^{-1} \delta_{j_v j'_v} \delta_{m_v m'_v}. \quad (7)$$

We consider the dipole transition from core  $4d$  states ( $j_c = 2 \pm 1/2$ ) to valence  $5f$  states ( $j_v = 3 \pm 1/2$ ). Using the relevant values of 6- $j$  symbol in eq. (5), the absorption intensity for each transition is given as

$$I_{3/2} = I(4d_{3/2} \rightarrow 5f_{5/2}) = \langle n_{5/2}^h \rangle (2l_v + 1)(l_v - 1)/l, \quad (8)$$

$$\begin{aligned} I_{5/2} &= I(4d_{5/2} \rightarrow 5f_{5/2}) + I(4d_{5/2} \rightarrow 5f_{7/2}) \\ &= \langle n_{5/2}^h \rangle / l_v + \langle n_{7/2}^h \rangle (2l_v - 1). \end{aligned} \quad (9)$$

The branching ratio for the  $4d \rightarrow 5f$  transition is given as

$$B = \frac{I_{5/2}}{I_{5/2} + I_{3/2}} = \frac{\langle n_{7/2}^h \rangle + \langle n_{5/2}^h \rangle / [l_v (2l_v - 1)]}{\langle n_{7/2}^h \rangle + \langle n_{5/2}^h \rangle}. \quad (10)$$

For the valence states of orbital angular moment  $l$ , the expectation value of the angular part of the spin-orbit interaction is related to the electron occupation numbers  $\langle n_{j_\pm} \rangle$  of the total angular momentum levels  $j_\pm = l \pm 1/2$ .

$$\begin{aligned} \sum_{i \in f} \langle \mathbf{l}_i \cdot \mathbf{s}_i \rangle &= \sum_{j=j_\pm} \langle n_j \rangle \left[ j(j+1) - l(l+1) - \frac{3}{4} \right] \\ &= -(l+1) \langle n_{j_-} \rangle + l \langle n_{j_+} \rangle. \end{aligned} \quad (11)$$

Using the definitions  $\langle n^h \rangle = \langle n_{5/2}^h \rangle + \langle n_{7/2}^h \rangle$  and eq. (11), the spin-orbit sum rule for  $4d \rightarrow 5f$  transition is given by

$$B = \frac{3}{5} - \frac{4}{15} \frac{1}{\langle n^h \rangle} \sum_{i \in 5f} \langle \mathbf{l}_i \cdot \mathbf{s}_i \rangle. \quad (12)$$

While we have made the assumption that the core electrons are localized, this assumption is not necessary for the valence  $f$  electrons. Therefore, under the conditions stated

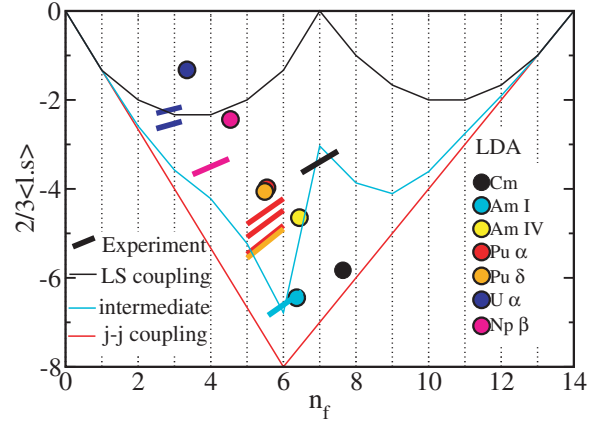


Fig. 2: The LDA expectation value of the angular part of the spin-orbit interaction. The LDA results are denoted by circles for actinide elements as a function of the  $5f$  electron count ( $n_f$ ). Paramagnetic phase is considered in all cases. Corresponding experimental data are denoted by the same color of dashes. The three common angular-momentum coupling schemes are shown:  $LS$ ,  $jj$ , and intermediate coupling schemes.

before, the sum rule is valid not only in atomic system but also in solid system, and the spin-orbit strength can be estimated from the partial occupancy of valence states at a given site, theoretically. It shows that the angular part of the spin-orbit strength is linearly related to the branching ratio in XAS and EELS [12,17–19]. One should note that this sum rule should be corrected when the core-valence interaction is increased [8].

To obtain the spin-orbit strength and branching ratio, we calculated the partial occupancies  $\langle n_{j_\pm} \rangle$  in solid system by using the LDA and LDA + DMFT method [21]. We use a relativistic version of the linearized muffin-tin orbital (LMTO) method for LDA calculations [22]. In the LDA + DMFT method, the itinerant  $spd$  electrons are treated using LDA, and the strongly correlated  $f$  electrons are considered in DMFT approach, which maps a lattice problem to a single-impurity problem in a self-consistent electronic bath [21,23]. To solve the impurity problem, we used the vertex corrected one-crossing approximation [21], and the results are further cross-checked by the continuous time quantum Monte Carlo method [24]. The Slater integrals  $F^k$  ( $k = 2, 4, 6$ ) and spin-orbit coupling constants are computed by Cowan's atomic Hartree-Fock (HF) program with relativistic corrections [25]. We scale the Slater integrals by 70% to account for the screening of the solid. We take Coulomb interaction  $U = 4.5$  eV for actinide elements and 8.0 eV for oxides. We used an  $fcc$  structure for Pu, Am, and Cm with corresponding volume of each phases, while  $\alpha$ - and  $\beta$ - phases are used for U and Np, respectively.

When the atomic interactions are turned off, the LDA + DMFT method reduces to the LDA method. Since there has not been a systematic study of how this method fares *vis à vis* the branching ratio, we include

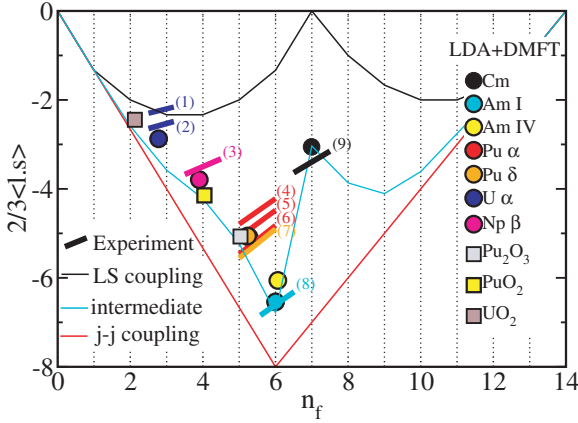


Fig. 3: The LDA + DMFT expectation value of the angular part of the spin-orbit interaction. The LDA + DMFT results are denoted by circles and rectangles for actinide elements and oxides, respectively. The experimental results obtained from EELS and XAS are denoted by thick dashes (1)–(8), because the number of electrons are not defined in the experiments. (1)  $\alpha$ -U XAS [26], (2)  $\alpha$ -U EELS [8,13], (3)  $\alpha$ -Np XAS [10], (4)  $\alpha$ -Pu XAS [8], (5)  $\alpha$ -Pu EELS [8], (6)  $\alpha$ -Pu EELS [13], (7)  $\delta$ -Pu EELS [13], (8) Am I EELS [11], (9) Cm EELS [11].

some LDA results in our study. In fig. 2, we show the spin-orbit strength of actinide elements obtained by the LDA method and compare to corresponding experimental data. We also show results for the three common angular-momentum coupling schemes: *LS* (Hund's rule is dominant), *jj* (spin-orbit interaction is dominant), and intermediate coupling scheme (obtained from isolated atomic limit). The intermediate coupling scheme shows a good agreement with experimental results of late actinide elements, Am and Cm. In ref. [11], the calculated value of Cm metal overestimates the experimental value. In our result, it shows better agreement with experiment because we scaled the Slater integrals by 70%, which slightly moves the intermediate coupling scheme toward the *jj* coupling scheme compared to the scaling of 80%. The conventional value 80% is reasonable approximation for very localized system such as oxides. However, smaller values are necessary for very itinerant systems. For example, for transition metal elements, the scaling factor is drastically decreased for better description of spectroscopy [27]. As pointed out by refs. [8,9] for  $\alpha$ -U, and ref. [10] for  $\alpha$ -Np, these metals deviate from the intermediate coupling scheme, which means these systems are delocalized and the effective spin-orbit strength decreases.

The LDA results are in overall disagreement with experimental data and the intermediate coupling scheme. From U to Pu the spin-orbit strength is much underestimated. Due to the overestimated band width of the LDA method, the spin-orbit strength of the actinide element is considerably suppressed compared to the atomic cases. Only Am is well described by the LDA method due to its special configuration. There is an optimal spin-orbit

stabilization of Am  $f^6$  configuration, which gives clear splitting of occupied  $j=5/2$  and unoccupied  $j=7/2$  states in the LDA density of states. Our results show that the LDA description of the branching ratio is not proper for actinide elements, as shown in fig. 2.

Figure 3 shows the spin-orbit strength obtained by the LDA + DMFT calculation. Our results are in good agreement with experimental results of all actinide elements. The branching ratio of late actinides, Am and Cm, are in good agreement with the intermediate coupling scheme as experimental data. In well localized system, only single atomic multiplet configuration is occupied and the system can be well approximated by an atomic problem, which is the intermediate coupling scheme. On the other hand, as the system is delocalized the  $f$  electrons become fluctuating between various atomic configurations and exchanging electrons with the surrounding medium. As a result, the spin-orbit strength is suppressed and the branching ratio moves from the intermediate scheme towards the *LS* coupling scheme. Note that the value for U and Np in fig. 3 is further away from the intermediate coupling scheme than late actinides. Also note that this is not a competition between the spin-orbit interaction and the Hund's rule coupling. This is the competition between the spin-orbit interaction and the delocalization. If the system is fully delocalized, the spin-orbit strength goes to zero and the branching ratio is just statistical value of  $3/5$ . According to our plot,  $\delta$ -Pu also deviates from the intermediate coupling scheme, hence this system is partly itinerant. This deviation becomes larger for earlier actinides such as Np and U.

Our results for U and Np slightly overestimate the spin-orbit strength measured in experiments. Here, we neglected the interference effect between different site in the description of core-valence transition as explained in eq. (4). In the impurity problem, we use the one-crossing approximation method, which might overestimate the localization of  $f$  electrons because it is based on the local atomic description. Also, the on-site Coulomb interaction  $U$  should be smaller than 4.5 eV for rather itinerant system,  $\alpha$ -U and  $\alpha$ -Np. By improving those effects, LDA + DMFT can give more delocalized branching ratio behavior.

We also investigate the change of spin-orbit strength under pressure, which are not available in atomic calculation. The volume of  $\alpha$ -Pu and Am IV is highly suppressed by 25% and 40% compared to the volume of  $\delta$ -Pu and Am I, respectively. The difference of  $n_f$  and the branching ratio between  $\alpha$ -Pu and  $\delta$ -Pu is almost negligible and hard to detect, similar to EELS experiments [13,15]. Although there is a significant change in the low-energy physics such as specific heat, the high energy probe of  $n_f$  and the branching ratio is rather insensitive to the degree of localization. On the other hand, there is a noticeable change between Am I and Am IV. There is a transition from optimal spin-orbit stabilization for  $f^6$  to optimal exchange interaction stabilization for  $f^7$  configuration [11]. This transition

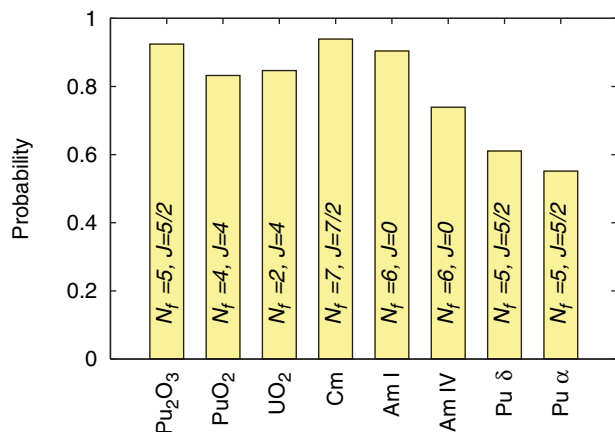


Fig. 4: Probability of the most occupied atomic ground-state multiplet. The height of the peak corresponds to the fraction of the time the  $f$  electrons of the solid spends in the given atomic multiplet, denoted by the  $5f$  electron count  $N_f$  and the total spin  $J$  of the atom.

induces a significant change in branching ratio between Am I and Am IV only with slight change of  $n_f$ .

The branching ratio shows systematic deviation from atomic calculation across the actinide series. Figure 4 shows the probability of the most occupied ground state multiplet for each elements. The branching ratio of Cm and Am are very close to the atomic case, because the probability of the  $f^7$  ( $f^6$ ) ground state is 95% (90%) in valence histogram [4], which reflects almost atomic ground states. As the atomic number is decreased, the system becomes delocalized, and the spin-orbit strength is decreased. In early actinides, the  $5f$  electrons are delocalized and they are distributed over various atomic configurations and not only in the ground state atomic multiplet. Note that  $\delta$ -Pu already shows deviation from localized states, as discussed in the suppressed spin-orbit strength of  $\delta$ -Pu. Under pressure, the  $5f$  electrons are delocalized, and the probability of atomic ground state multiplet is decreased as shown in Am IV and  $\alpha$ -Pu.

Finally we also study actinide oxide systems  $\text{Pu}_2\text{O}_3$ ,  $\text{PuO}_2$ , and  $\text{UO}_2$ . These materials are very important because they are used in nuclear fuels for energy generation. LDA + DMFT predicts that these materials are localized. As shown in fig. 3 their branching ratios are consistent with the intermediate coupling scheme. The calculated  $n_f$  indicates that trivalent metal ion in  $\text{Pu}_2\text{O}_3$  and tetravalent metal ion in  $\text{PuO}_2$  and  $\text{UO}_2$ , which shows that these systems can be described by ionic system rather than metallic or covalent system. Recent experiments on the  $4d \rightarrow 5f$  transition in EELS show that the branching ratio of  $\text{UO}_2$  and  $\text{PuO}_2$  are similar to that of  $\alpha$ -U and  $\delta$ -Pu, respectively, and it has been suggested that these actinide dioxides have covalent

metal-oxide bonding, and the number of  $f$  electrons can become non-integer number [13]. However, unpublished EELS results of the  $5d \rightarrow 5f$  transition in  $\text{UO}_2$  and  $\text{PuO}_2$  suggest the bonding is indeed ionic with a near integer change in  $5f$  occupancy [28]. So, further experimental work is required to investigate why the  $5d$  and  $4d$  spectra show ionic and covalent bonding nature, respectively.

\*\*\*

We acknowledge useful discussions with K. T. MOORE.

## REFERENCES

- [1] ARKO A. J. *et al.*, *Phys. Rev. B*, **62** (2000) 1773.
- [2] TOBIN J. G. *et al.*, *Phys. Rev. B*, **68** (2003) 155109.
- [3] GOUDER T. *et al.*, *Phys. Rev. B*, **71** (2005) 165101.
- [4] SHIM J. H., HAULE K. and KOTLIAR G., *Nature*, **446** (2007) 513.
- [5] SHICK A. *et al.*, *EPL*, **77** (2007) 17003.
- [6] ZHU J. X. *et al.*, *Phys. Rev. B*, **76** (2007) 245118.
- [7] MARIANETTI C. A., HAULE K., KOTLIAR G. and FLUSS M. J., *Phys. Rev. Lett.*, **101** (2008) 056403.
- [8] VAN DER LAAN G. *et al.*, *Phys. Rev. Lett.*, **93** (2004) 097401.
- [9] TOBIN J. G. *et al.*, *Phys. Rev. B*, **72** (2005) 085109.
- [10] MOORE K. T., VAN DER LAAN G., WALL M. A., SCHWARTZ A. J. and HAIRE R. G., *Phys. Rev. B*, **76** (2007) 073105.
- [11] MOORE K. T. *et al.*, *Phys. Rev. Lett.*, **98** (2007) 236402.
- [12] VAN DER LAAN G. and THOLE B. T., *Phys. Rev. B*, **53** (1996) 14458.
- [13] MOORE K. T. *et al.*, *Phys. Rev. B*, **73** (2006) 033109.
- [14] BUTTERFIELD M. T., MOORE K. T., VAN DER LAAN G., WALL M. A. and HAIRE R. G., *Phys. Rev. B*, **77** (2008) 113109.
- [15] MOORE K. T. and VAN DER LAAN G., arXiv:0807.0416 (2008).
- [16] MOORE K. T. *et al.*, *Philos. Mag.*, **84** (2004) 1039.
- [17] THOLE B. T. and VAN DER LAAN G., *Phys. Rev. B*, **38** (1988) 1358.
- [18] VAN DER LAAN G. and THOLE B. T., *Phys. Rev. Lett.*, **60** (1988) 1977.
- [19] THOLE B. T. and VAN DER LAAN G., *Phys. Rev. A*, **38** (1988) 1943.
- [20] VAN DER LAAN G., *Phys. Rev. B*, **57** (1998) 112.
- [21] KOTLIAR G. *et al.*, *Rev. Mod. Phys.*, **78** (2006) 865.
- [22] SAVRASOV S. Y., *Phys. Rev. B*, **54** (1996) 16470.
- [23] GEORGES A., KOTLIAR G., KRAUTH W. and ROZENBERG M. J., *Rev. Mod. Phys.*, **68** (1996) 13.
- [24] HAULE K., *Phys. Rev. B*, **75** (2007) 155113.
- [25] COWAN R. D., *The Theory of Atomic Structure and Spectra* (University of California Press, Berkeley) 1981.
- [26] KALKOWSKI G., KAINDL G., BREWER W. D. and KRONE W., *Phys. Rev. B*, **35** (1987) 2667.
- [27] VAN DER LAAN G., *Phys. Rev. B*, **51** (1995) 240.
- [28] MOORE K. T., private communication.